THE EFFECT OF NANOSTRUCTURE UPON THE DEFORMATION MICROMECHANICS OF CARBON FIBRES

F. Tanaka[1,2,3], T. Okabe[1], H. Okuda[2], M. Ise[2], I. A. Kinloch[3], R. J. Young[3*]

[1] *Department of Aerospace Engineering, Tohoku University, 6-6-01 Aoba-yama, Aoba-ku, Sendai, 980-8579, Japan*
[2] *Composite Materials Research Laboratories, TORAY Industries, Inc., 1515 Tsutsui, Masaki-cho, Iyo-gun, Ehime, 791-3193, Japan*
[3] *School of Materials, University of Manchester, Grosvenor Street, Manchester, M1 7HS, UK*
** robert.young@manchester.ac.uk*

Keywords: carbon fibres, Young's modulus, micromechanics, amorphous carbon.

Abstract
We have introduced the Mori-Tanaka theory as a new micromechanical model to predict the Young's modulus for carbon fibres, that takes into account both the crystallites and amorphous components of the carbon fibre structure. The axial elastic constants of the bulk carbon fibres were measured directly by X-ray diffraction (XRD) and an axial shear modulus of about 20 GPa was calculated. The elastic constants of the amorphous carbon in the fibres and the volume fractions of crystallites were estimated using micromechanical models. It was found that the amorphous modulus was approximately 200 GPa and the volume fractions of crystallites were 0.4 to 0.8, depending upon the nanostructure of the carbon fibres. Also, as it is known that the Raman G band shift rate per unit strain is related to the crystallite modulus, the data indicated a nearly constant value of 1.1 TPa, consistent with direct measurements upon graphene. The results show clearly that the behavior of carbon fibres can be expressed through a composite mechanical model that assumes they consist of both crystalline and amorphous carbon components.

1 Introduction
Polyacrylonitrile (PAN)-based carbon fibres were first developed in 1959 [1] and now play an important role in producing light-weight structural materials. In order to optimize and improve the properties of carbon fibres, it is important to understand the factors that control their Young's modulus. A number of studies have already been undertaken on relationships between the mechanical properties and structure. The structure and morphology of carbon fibers has been investigated and detailed accounts have been given by Oberlin, [2] Johnson [3-4] and Donnet. [5] Various mechanical models of carbon fibres were originally introduced in order to explain quantitatively the relationships between the tensile modulus and the crystallite orientation: the uniform stress model and the mosaic model, both consisting simply of aligned crystallites perfectly connected with each other. The uniform stress model is able to predict the behaviour of graphitized carbon fibres and implies the importance of the axial shear modulus upon the bulk carbon fibre modulus, such as rayon-based and pitch-based carbon fibres. [6-7] More recently, it was suggested that a more precise model was needed to be used for PAN-based carbon fibres and it was shown that the mosaic model, a type of

series-parallel model, could explain the measured increases in the tensile modulus and the crystallite orientation with tensile stress. [8] Moreover, in-situ tensile tests of single carbon fibres by X-ray diffraction revealed that the axial elastic constants (of the crystallites), which increased with fibre modulus, [9] did not correspond with the values observed in previous work which found them to be independent of fibre modulus.[8] Previous Raman spectroscopic analysis of carbon fibres revealed that the G and G' peak shift rates per unit applied strain for carbon fibres exhibited a nearly linear relationship with the tensile modulus, [10-11] and we will show that this suggests a constant crystallite modulus within the fibres. Yet, the G band shift rates vary with the various production conditions of fibres despite the fibres having the same diameter and Young's modulus. This suggests that the crystallite modulus or the stress experienced by the crystallites varies. [12] It has been demonstrated, however, that such the previous models [6-9] are unable to predict the behaviour of low modulus PAN-based carbon fibres since the models are too simplified and ignore factors such as the disordered structure within the fibres. We have therefore introduced a new micromechanical model to predict the Young's modulus of carbon fibres, which takes into account the properties of both the crystalline and amorphous components of the carbon fibre structure.

2 Theory

In this section, we describe the micromechanical model to determine the elastic constants of the two components of the carbon fibres, crystallites and amorphous carbon. For this reason, we derive a composite model which takes into account both the crystalline and amorphous components. The combination of Eshelby's solution [13] and Mori-Tanaka's average stress [14] could calculate the elastic coefficients. The elastic constants of the bulk carbon fibres $\bar{\mathbf{C}}$ in the direction of the oriented crystallite long axis can be derived as

$$\bar{\mathbf{C}} = \left[\left\{\mathbf{I} + f(1-f)(\mathbf{C}^* - \mathbf{C}^0)(\mathbf{S} - \mathbf{I}) + \mathbf{C}^*\right\}^{-1}(\mathbf{C}^0 - \mathbf{C}^*)\left(\mathbf{C}^0\right)^{-1}\right]^{-1} \quad (1)$$

where $\mathbf{C}^0$ and $\mathbf{C}^*$ are the elastic coefficient of the amorphous carbon and the crystallite carbon in the fibres, respectively, f is the volume fraction of the crystallite carbon, $\mathbf{I}$ is the kronecker delta and $\mathbf{S}$ is Eshelby tensor which depends upon the shape of the crystallites. We have assumed that (1) the amorphous carbon is isotropic with a Poisson's ratio of 0.3, (2) the elastic coefficients of the crystallite are same as those of graphite, [15] (3) the total volume fraction of crystallite and amorphous carbon is equal to unity and (4) the shape of the crystallites, based on a TEM image of a typical PAN-based carbon fibre (Fig.1), is an oblate spheroid and the aspect ratio of the oblate spheroid/ellipse is the ratio of the crystallite diameter L_a to thickness L_c, determined by X-ray diffraction (XRD). Although the detailed shape of the crystallites is unclear, it is thought that the crystallites are equivalent to oblate spheroids with the carbon layer axis parallel to their long axes. The long axes of the spheroids will also have an orientation distribution because there is a crystallite orientation distribution.

In addition, considering the orientation distribution, $\bar{\mathbf{C}}$ is converted in the direction of the fibre axis to coincide with the principle axis of stress. Since we do not consider the transverse elastic constants of the bulk fibres in this study, the tensor transformation is converted two-dimensionally.

$$\bar{\mathbf{C}}' = \mathbf{R}^{-1}\bar{\mathbf{C}}\mathbf{R} \quad (2)$$

where **R** is the coordinate transformation matrix which has the orientation angle φ between the normal of the carbon layer and the fibre axis. The orientation angle distribution is determined by XRD. Based on XRD, the components of the compliance tensor of the bulk fibres in the direction of crystallite orientation axis, $s_{11}(=1/e_1^f)$ and $s_{44}(=1/g^f)$, are used in this study.

Next, we explain the calculation methods of the stress and the strain within the crystallites and the amorphous carbon that will be used to check the deformation of the crystallites and the amorphous carbon experimentally. In order to consider the orientation distribution, the stress within the individual declined crystallite is summed. The stress within the crystallite $\langle\boldsymbol{\sigma}\rangle_I$ and the amorphous carbon $\langle\boldsymbol{\sigma}\rangle_M$ and the total strain within the crystallite $\langle\boldsymbol{\gamma}\rangle_I$ and the amorphous carbon $\langle\boldsymbol{\gamma}\rangle_M$ can be written as,

$$\langle\boldsymbol{\sigma}\rangle_I = \sum\langle\boldsymbol{\sigma}(N)\rangle_I / M \qquad (N=1, 2, 3, \ldots M) \tag{3}$$

$$\langle\boldsymbol{\sigma}\rangle_M = \frac{\boldsymbol{\sigma}^0 - f\langle\boldsymbol{\sigma}\rangle_I}{1-f} \tag{4}$$

$$\langle\boldsymbol{\gamma}\rangle_I = \sum\mathbf{C}^{*-1}(N)\langle\boldsymbol{\sigma}(N)\rangle_I / M \tag{5}$$

$$\langle\boldsymbol{\gamma}\rangle_M = \sum\mathbf{C}^{0^{-1}}\langle\boldsymbol{\sigma}\rangle_M \tag{6}$$

where M is the total number of the crystallites, $\langle\boldsymbol{\sigma}(N)\rangle_I$ is the individual stress within the crystallite, written as [14]

$$\langle\boldsymbol{\sigma}(N)\rangle_I = \mathbf{C^0}(\mathbf{S}-\mathbf{I})\boldsymbol{\varepsilon}^* - f\mathbf{C^0}(\mathbf{S}-\mathbf{I})\boldsymbol{\varepsilon}^* \tag{7}$$

where $\boldsymbol{\sigma^0}$ is the applied stress in the fibres (σ_{11}^0=1) and $\boldsymbol{\varepsilon}$* is eigenstrain, and is given as

$$\boldsymbol{\varepsilon}^* = \left\{(1-f)(\mathbf{C}^{*\prime}-\mathbf{C}^0)(\mathbf{S}-\mathbf{I}) + \mathbf{C}^{*\prime}\right\}^{-1}(\mathbf{C}^0 - \mathbf{C}^{*\prime})\mathbf{C}^{0^{-1}}\boldsymbol{\sigma}^0 \tag{8}$$

In order to consider the orientation distribution, $\mathbf{C}^*$ is converted into $\mathbf{C}^{*\prime}$ using same method as in eq.(2). It should be noted that in this case the simplified Eshelby tensor in Eq. (1) is modified to take into account crystallite orientation

3 Experimental

3.1 Materials

In order to follow the dependence of the mechanical properties of the carbon fibres upon nanostructure, we prepared five different types of PAN-based carbon fibres, with Young's moduli in the range 200~500 GPa (Table 1). It was found that the values of the aspect ratio, L_a / L_c, were in the range 1.2~2.4, consistent with Oya's data. [16]

3.2 Methods

The specimens were prepared using a 2 mm thick poly-(methyl methacrylate) beam and each single fibre was embedded on the surface of the beam for Raman analysis. A thin layer of

PMMA was then coated on top of the beam. The PMMA beam was deformed in 4-point bending and the strain monitored using a strain gauge attached to the beam surface. A well-defined Raman spectrum could be obtained through the PMMA coating using a low-power He-Ne laser (1.96 eV and <1mW at the sample in a Renishaw 2000 spectrometer) and the deformation of the fibre in the composite was followed from the shifts of the G and D bands. Five measurements from different fibres were averaged for each type of fibres. The laser beam polarization was always parallel to the tensile axis. For XRD, an epoxy resin impregnated carbon fibres bundle of about 300 fibres was prepared. The experiment was performed at the beam line (BL03XU) of the Japanese Synchrotron Radiation Facility (SPring-8). The load was increased stepwise, and for each loading step, two main parameters, the 10 and 002 reflections were evaluated from the 2D diffraction patterns. The position of the 10 reflection gives the in-plane distance d10 of the carbon atoms in loading direction and the azimuthal width (half width at half maximum) of the 002 reflection describes the orientation of the crystallites with respect to the fiber axis.

Table 1. Physical and mechanical properties of the carbon fibres

Fibre	Young's modulus* /GPa	L_a /nm	L_c /nm	Aspect ratio	$\langle \cos^2 \varphi \rangle$	Diameter /μm	Density /g/cm^3
1000ºC	220	1.9	1.6	1.18	0.067	5.8	1.78
T800G	255	2.6	2.0	1.30	0.064	5.5	1.80
M30S	261	3.8	2.4	1.59	0.057	5.6	1.73
M40S	360	8.1	3.8	2.12	0.042	5.4	1.80
M50S	440	13.5	5.8	2.33	0.026	5.3	1.90

* The initial Young's modulus ($\sigma \rightarrow 0$)

Next, we describe the evaluation of $\bar{\mathbf{C}}$. A formula for the axial elastic constant of the bulk fibre is derived using the generalized Hooke's law and tensor transformation

$$\frac{1}{E^f} = \frac{1}{e_1^f} + \left(\frac{1}{g^f} - \frac{2}{e_1^f} - \frac{2\nu_{13}^f}{e_3^f} \right) \cos^2 \varphi + \left[-\frac{1}{g^f} + \frac{1}{e_1^f} + \frac{\left(1 + 2\nu_{13}^f\right)}{e_3^f} \right] \cos^4 \varphi \tag{9}$$

where E^f is the Young's modulus of the bulk carbon fibres, $s_{11}(=1/e_1^f)$, $s_{13}(=\nu_{13}/e_3^f)$, $s_{33}(=1/e_3^f)$ and $s_{44}(=1/g^f)$ are the components of the compliance tensor of the bulk carbon fibres in the direction of crystallite orientation axis. For the evaluation of the e_1^f, the strain of the bulk carbon fibres along the direction of the crystallite orientation axis (ε_1^f) is obtained from the shift of the lattice spacing d_{10} by XRD under the applied stress.

$$\varepsilon_1^f = \frac{d_{10}(\sigma) - d_{10}(0)}{d_{10}(0)} \tag{10}$$

The graphite 10 lattice band signal is obtained from the graphene planes, consisting of both highly-ordered crystallites and small pieces of sp^2 structure in amorphous sp^2/sp^3 complex carbon, not just from that in the crystallite.

The axial elastic constant of the bulk carbon fibres (e_1^f) is then calculated from the slope of the stepwise applied stress in the bulk fibres versus the 10 strain curve [9], considering the orientation angle.

$$1/e_1^f = \Delta\varepsilon_1^f / \Delta\sigma \langle \cos^2 \varphi \rangle \tag{11}$$

The orientation distribution parameter $\langle \cos^2 \varphi \rangle$ of the orientation angle φ of the between the normal of the carbon layer and the fibre axis can be approximated by same method as in previous work. [9] Using eq. (9), the shear modulus of the bulk carbon fibres (g^f) is then calculated. The e_3^f and ν_{13} values were approximated as 44.6 GPa and 0.023 in this study and assumed to be equal to the values of graphite. [15] Now, substituting the e_1^f and g^f into eq. (1), the amorphous modulus component of the stiffness tensor, $\mathbf{C^0}$, and the crystallinity, f, is calculated.

4 Result and Discussion

In order to determine the axial elastic constants of the bulk carbon fibres (e_1^f), the strains in the bulk carbon fibres along the direction of the crystallite orientation axis were measured first of all, directly by XRD using Eq. (10) through the stepwise application of stress upon fibre bundles. Values of e_1^f in the range 0.3~0.8 TPa were obtained from Eq. (11) (Table 2), depending upon the fibre structure.

Table 2. Calculated results of the axial elastic constant and axial shear modulus for the bulk carbon fibres.

Fibre	Young's modulus /GPa	e_1^f /GPa	g^f /GPa
1000ºC	220	333	24.9
T800G	255	434	27.1
M30S	261	454	22.0
M40S	360	579	18.4
M50S	440	739	11.2

Using to Eq. (9) and the measured value of e_1^f, an axial shear modulus of the bulk carbon fibres (g^f) of about 20 GPa was calculated for all fibres (Table 2), and this is similar to that found by others in previous studies. [8]

Next, the elastic constants of the amorphous carbon in the fibres and the volume fractions of crystallites (= degree of crystallinity) were estimated using the Mori-Tanaka micromechanical models (Table 3). The only two unknown parameters, the amorphous modulus component of the stiffness tensor, $\mathbf{C^0}$, and the crystallinity, f, can be calculated to match the two given parameters, e_1^f and g^f of the bulk fibres using Eqs. (1) and (9). It was found that the amorphous modulus was approximately 0.2 TPa and the volume fractions of crystallites were 0.4 to 0.8, depending upon the nanostructure of the carbon fibres. The internal stresses on the crystallites and amorphous carbon were calculated to be 1.1~1.2 times and 0.6~0.9 times the applied stress of the carbon fibres, respectively from Eqs. (3), (4) and (7). It appears that this is because, in spite of the large difference of modulus between crystallite and amorphous carbon, the aspect ratio of the crystallites is relatively small. Also, the total strain within the crystallites and amorphous carbon were calculated from Eqs. (5), (6) and (7), naturally indicating a significantly higher strain in the amorphous carbon than in the crystallites.

The deformation of the different components in the bulk carbon fibres, i.e. the crystallites and the amorphous carbon was also followed using Raman spectroscopy. Specifically, in the case of carbon fibres, the shift of the G band with stress reflects the in-plane deformation of the graphene layers crystallites only.[17] The carbon fibres studied gave well-defined Raman

spectra characteristic of carbon materials with a G band, a D' band and a D band. We used Raman spectroscopy to follow the crystallite deformation from the shift of the G band in fibres in a model composite consisting of a thin polymer matrix layer and a single fibre. It was found that the G band shift showed a non-linear behaviour with strain as the beam was deformed in bending. This reflects the non-linear stress-strain curves of the fibres, with modulus hardening in tension and modulus softening in compression. [8] The initial shift rates per unit strain ($\varepsilon^f \rightarrow 0$) are shown as a function of fibre modulus in Fig. 1. It can be seen that the G band shift rate increases approximately linearly with fibre modulus.

Table 3. Calculated results of the properties of the crystallites and amorphous material

Fibre	Amorphous modulus /GPa	Crystallinity	$\langle\sigma_{11}\rangle_I$ /times	$\langle\sigma_{11}\rangle_M$ /times	$\langle\gamma_{11}\rangle_I$ /GPa^{-1}	$\langle\gamma_{11}\rangle_M$ / GPa^{-1}
1000ºC	159	0.458	1.22	0.82	0.0031	0.0052
T800G	200	0.508	1.18	0.81	0.0028	0.0041
M30S	186	0.551	1.19	0.76	0.0029	0.0041
M40S	211	0.633	1.18	0.68	0.0025	0.0033
M50S	212	0.770	1.12	0.60	0.0021	0.0029

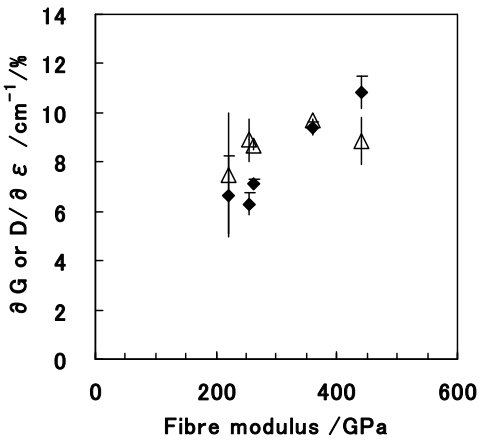

Fig. 1 Dependence of the shift rates for the G (◆) and D (Δ) bands upon tensile modulus for the PAN-based carbon fibres.

The dependence of the band shift ($\Delta G/\Delta\varepsilon^f$) upon fibre modulus, E^f, now needs to be reconsidered. The inverse slope of the plot in Fig. 1 is related to the applied stress in "the bulk fibre" (σ^f) divided by the in-plane deformation of the graphene layers crystallites only (ε^c), as shown below in Eq. (11).

$$\frac{E^f}{\Delta G/\Delta\varepsilon^f} = \frac{\Delta\sigma^f}{\Delta\varepsilon^f} \times \frac{\Delta\varepsilon^f}{\Delta G} = \frac{\Delta\sigma^f}{\Delta G\left(\propto \Delta\varepsilon^c\right)} \tag{11}$$

The crystallite modulus E^c, can then be determined from this relationship using the internal stress within the crystallite $\langle\sigma_{11}\rangle_I$ ($= \Delta\sigma^c / \Delta\sigma^f$) as follows

$$\frac{\Delta\sigma^f}{\Delta\varepsilon^c} \times \frac{\Delta\sigma^c}{\Delta\sigma^f} = \frac{\Delta\sigma^c}{\Delta\varepsilon^c} = E^c \tag{12}$$

The deformation of the crystallites was calculated using the value of the in-plane elongation per unit of Raman G band shift, $\Delta G/26$ cm^{-1}/% = $\Delta\varepsilon^c$, according to the average deformation data of graphene G^+/G^- band. [18] The calculated crystallite modulus from Eq. (12) for all fibres was a nearly constant value of 1.1 TPa (Fig. 2), consistent with direct measurements upon graphene. [19]

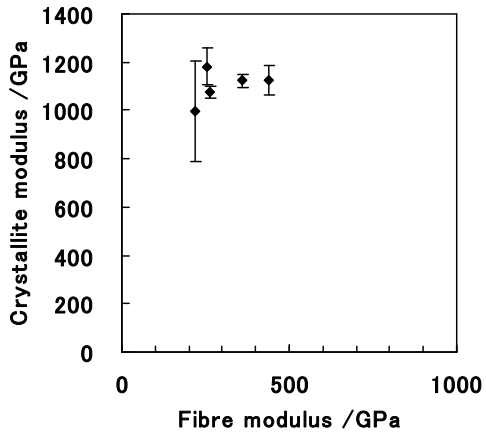

Figure 2. The calculated crystallite modulus as a function of the fibre modulus.

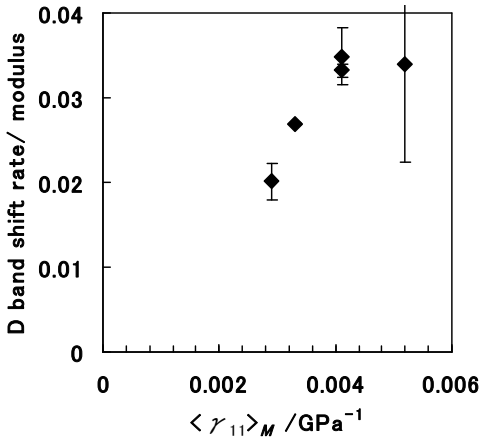

Figure 3. The value of D band shift rate /fibre modulus as a function of the calculated total strain in the amorphous carbon

In contrast, the D band reflects the A_{1g} vibrations of sp^2 carbon which are from edge or lattice defects of the crystallites and low molecular weight poly-aromatic carbon components in the amorphous carbon. Therefore, it was assumed that D band shift reflected the average deformation of the amorphous carbon, consisting of sp^2 and sp^3 carbon. The initial D shift rates per unit strain ($\varepsilon^f \rightarrow 0$) are shown in Fig. 1. It can be seen that the rate gives higher deformation than the G-band rate for low modulus type fibres and lower for high modulus type fibres. Considering the plots as well as the G band, it appears that the values of D band shift rate divided by the fibre modulus ($\Delta D/\Delta\sigma^f$) were related to the total strain within the amorphous carbon in case of applying $\Delta\sigma^f$.

$$\frac{\Delta D}{\Delta \varepsilon^f} \times \frac{\Delta \varepsilon^f}{\Delta \sigma^f} = \frac{\Delta D\left(\propto \varepsilon^a\right)}{\Delta \sigma^f} \qquad (13)$$

The rearranged values ($\Delta D/\Delta\sigma^f$) were plotted against the total strain within the amorphous carbon $\langle \gamma \rangle_M$ calculated by the Mori-Tanaka theory (Fig. 3). According to the good agreement between the Raman data and the results of the calculation, it is suggested that the D band shift is related to the deformation of the amorphous carbon component.

It has been demonstrated that during the deformation of bulk carbon fibres, the detailed deformation of the crystallites and the amorphous carbon can be followed using X-ray diffraction and Raman spectroscopy. The results show clearly that the behaviour of carbon fibres can be expressed through a composite mechanical model that assumes they consist of both crystallites and amorphous carbon. Also, it is confirmed that the Young's moduli of the crystallite and the amorphous carbon are approximately 1.1 TPa and 0.2 TPa, respectively and the fibre modulus depends on the degree of crystallinity (controlled by maximum carbonization temperature). Finally, our new micromechanical model based upon the Mori-Tanaka theory can be used to predict the Young's modulus for carbon fibres. This present

study has important implications for understanding the structural parameter that control the Young's modulus of PAN-based carbon fibres, such as the amorphous modulus and crystallinity. Carbon fibres have an impressive level of mechanical properties, that are controlled the mixture of sp^2 and sp^3 carbon components at the nano-scale. We believe that there is still considerable scope for improving mechanical properties, such as the Young's modulus, using the knowledge gained in this study.

References

[1] Patent announcement Japan, Shouwa- 37-4405［in Japanese］
[2] A. Oberlin, Carbonization and graphitization, *Carbon*, **22**, pp. 521-541, (1984).
[3] D. J. Johnson, Structure-property relationships in carbon fibres, *J. Phys. D.: Appl. Phys.*, **20**, pp. 286-291 (1987).
[4] D. J. Johnson, *Chapter 1*, In Chemistry and Physics of Carbon, **20**, pp. 1-58, Marcel Dekker, New York, (1987).
[5] J. B. Donnet and R. C. Bansal, In Carbon Fibers, 2nd Ed., **51**. Marcel Dekker, New York, (1990).
[6] W. Ruland, The relationship between preferred orientation and Young's modulus of carbon fibers, *Applied Polymer Symposia*, **9**, pp. 293-301 (1969).
[7] M. G. Northolt, L. H. Veldhuizen, H. Jansen, Tensile deformation of carbon fibers and the relationship with the modulus for shear between the basal planes, *Carbon*, **29**, 1267-1279 (1991).
[8] M. Shioya, E. Hayakawa, A. Takaku, Non-hookean stress-strain response and changes in crystallite orientation of carbon fibres, *J. Mat. Sci.*, **31**, pp. 4521-4532 (1996).
[9] D. Loidl, H. Peterlik, M. Muller, C. Riekel, O. Paris, Elastic moduli of nanocrystallites in carbon fibers measured by in-situ X-ray microbeam diffraction, *Carbon*, **41**, pp. 563-570 (2003).
[10] Y. Huang, R. J. Young, Effect of fibre microstructure upon the modulus of PAN- and pitch-based carbon fibres, *Carbon*, **33**, 97-107 (1995).
[11] C.A. Cooper, R.J. Young, M. Halsall, Investigation into the deformation of carbon nanotubes and their composites through the use of Raman spectroscopy, *Composites: Part A*, **32**, pp. 401-411 (2001).
[12] N. Melantis, P. L. Tetlow, C. Galiotis, S. B. Smith, Compressional behaviour of carbon fibres, *J. Mater. Sci.*, **29**, pp. 786-799 (1994).
[13] J. D. Eshelby, The Determination of the Elastic Field of an Ellipsoidal Inclusion, and Related Problems, *Proc. R. Sot. (A)*, **241**, pp. 376-396, (1957).
[14] T. Mori, K. Tanaka, Average stress in matrix and average elastic energy of materials with misfitting inclusions, *Acta Metallurgica*, **21**, pp. 571-574, (1973).
[15] G. B. Spence, Proceedings of the Fifth Conference on Carbon, **2**, pp. 531, (1961). (Pergamon Press, Inc., New York)
[16] N. Oya, D. J. Johnson, Longitudinal compressive behaviour and microstructure of PANbased carbon fibres, *Carbon*, **39**, pp. 635-645 (2001).
[17] A. Ferrari, Raman spectroscopy of graphene and graphite: Disorder, electron–phonon coupling, doping and nonadiabatic effects, *Solid State Communications*, 143, pp. 47-57 (2007).
[18] O. Frank, G. Tsoukleri, I. Riaz, K. Papagelis, J. Parthenios, A. C. Ferrari, A. K. Geim, K. S. Novoselov, C. Galiotis, Development of a universal stress sensor for graphene and carbon fibres, *Nature Communications*, **2**:255 DOI: 10.1038/ncomms1247, pp.1-7 (2011).
[19] C. Lee, X. Wei, J. W. Kysar, J. Hone, Measurement of the Elastic Properties and Intrinsic Strength of Monolayer Graphene, *Science*, **321**, pp. 385-388 (2008).